Supporting Information for

Disentangling the effects of external perturbations on coexistence and priority effects

Chuliang Song[1], Rudolf P. Rohr[2], David Vasseur[4], Serguei Saavedra[1]

[1]Department of Civil and Environmental Engineering, MIT,
77 Massachusetts Av., 02139 Cambridge, MA, USA

[2]Department of Biology – Ecology and Evolution, University of Fribourg,
Chemin du Musée 10, CH-1700 Fribourg, Switzerland

[3]Department of Ecology and Evolutionary Biology, Yale University,
New Haven, CT 06520, USA

A Equivalent parameterizations

It is worth noting that several mathematically equivalent parameterizations have been used to describe the LV dynamics of 2-competing species (Case, 2000). Yet, regardless of model parameterization, the conditions leading to coexistence or priority effects are equivalent under the Structural Approach. For example, in addition to the $\boldsymbol{r}$ formalism (Eq. 1) and MCT formalism (Eq. 4), the LV model can also be expressed in terms of carrying capacities (Vandermeer, 1975). In this other parameterization—what is known as the $\boldsymbol{K}$-formalism, the carrying capacities K_i are made explicit in the model as

$$\begin{cases} \dfrac{dN_1}{dt} = N_1 \dfrac{r_1}{K_1}(K_1 - N_1 - a_{12}N_2) \\ \dfrac{dN_2}{dt} = N_2 \dfrac{r_2}{K_2}(K_2 - a_{21}N_1 - N_2). \end{cases} \tag{S1}$$

Recall that the carrying capacity K_i of species i is computed as $K_i = r_i/\alpha_{ii}$. It corresponds to the abundance at equilibrium when the species grows in the absence of competition strength. Note that the carrying capacity is well defined only if $r_i > 0$, i.e., the species can grow in monoculture (Gabriel *et al.*, 2005). To be equivalent to Eq. (1), the competition strength must be standardized by the intraspecific competition, i.e., $a_{ij} = \alpha_{ij}/\alpha_{ii}$. Note that a_{ij} is traditionally called the niche overlap of species j on species i (Case, 2000). In the $\boldsymbol{K}$-formalism, the condition for coexistence (Eq. 2) reads as

$$\rho < \frac{K_2}{K_1}\sqrt{\frac{a_{12}}{a_{21}}} < \frac{1}{\rho}, \tag{S2}$$

and the condition for priority effects reads as

$$\rho > \frac{K_2}{K_1}\sqrt{\frac{a_{12}}{a_{21}}} > \frac{1}{\rho}. \tag{S3}$$

These two sets of inequalities are very similar to those in the $\boldsymbol{r}$-formalism (Eqs. 2 and 3). Notice that r_i is replaced by K_i and Q_j by a_{ij}. Replacing the new parametrization into Eqn. 5, the niche overlap is given by $\rho = \sqrt{a_{12}a_{21}}$, which reveals that the *niche overlap* ρ defined in MCT is, in fact, the geometric average of the niche overlap a_{ij} of the two competing species.

Thus, the representation of the dynamical behavior of the LV model can be drawn in the 2-dimensional space made by the species fitness ($\kappa_i = r_i/\sqrt{\alpha_{ii}\alpha_{ij}}$), the carrying capacities ($K_i = r_i/a_{ii}$), or the intrinsic growth rates (r_i) (Case 1999; Fig. S1). These representations in the space of intrinsic growth rates are the core concept behind the structural approach (Saavedra *et al.*, 2017b). That is, Figure S1 shows that all these representations are conceptually equivalent to describe the range (as an algebraic cone) of intrinsic growth rates leading to a given qualitative behavior (either coexistence or priority effects).

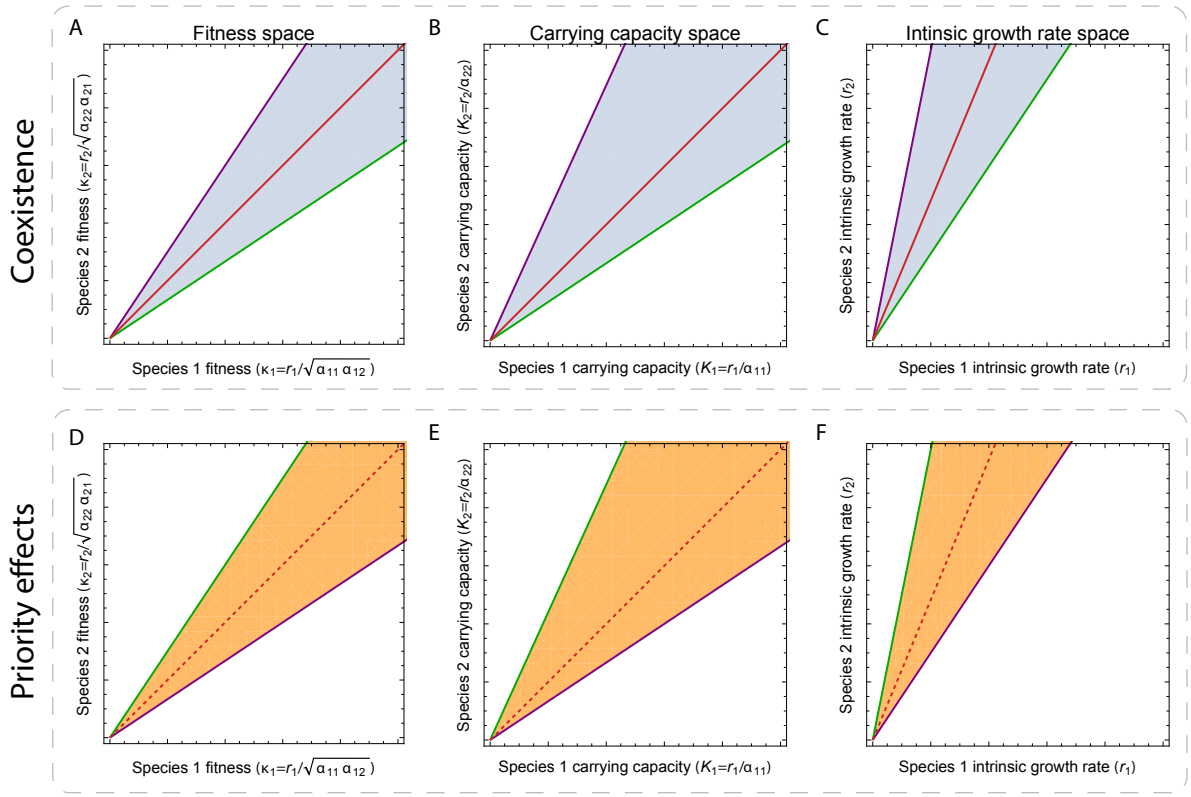

Figure S1: Space of intrinsic growth rates for coexistence and priority effects. The dynamics correspond to the Lotka-Volterra model (Eq. 1). These panels represent the range of intrinsic growth rates—species fitness (panels A and D), carrying capacities (panels B and E), and intrinsic growth rates (panels C and F)—leading to coexistence or priority effects. Whether we can be in the presence of coexistence or priority effects is determined by the stability-instability inequality, i.e., $\alpha_{22}/\alpha_{12} > \alpha_{21}/\alpha_{11}$ for coexistence (panels A and C) or $\alpha_{22}/\alpha_{12} < \alpha_{21}/\alpha_{11}$ for priority effects (panels D and F). The slopes (α_{21}/α_{11} in green and α_{22}/α_{12} in purple) of the two lines determining the coexistence (or priority effects) cone are computed from the competition strengths. Actually, these four panels are a simple geometric representation of the inequalities expressed in Eqs. (2) and (3). The red line represents the fitness equivalence line, and in dashed, its extension to priority effects.

B Importance of intrinsic growth rates

In the MCT formalism (Eq. 4), intrinsic growth rates do not play any explicit role in either feasibility nor stability. However, this is a special property of 2-species ODEs guaranteed by the Poincaré–Bendixson theorem (Strogatz, 2014). Yet, a well-known counter-example to the fact that intrinsic growth rates do impact the dynamics in other dimensions is the discrete logistic growth dynamics of a single species,

$$N_{t+1} = rN_t(1 - N_t), \tag{S4}$$

where increasing the intrinsic growth rate r would move the system from staying at a fixed equilibrium to a chaotic dynamics. Moreover, it is rather easy to show counter-examples in systems with more than 2 species. For example, consider the following 4-species competition ODEs with fixed interaction matrix (written following MCT formalism). The governing population dynamics are (Vano *et al.*, 2006)

$$\frac{d\mathbf{N}}{dt} = \text{diag}(\mathbf{r})\text{diag}(\mathbf{N})(1 - \begin{pmatrix} 1 & 1.09 & 1.52 & 0 \\ 0 & 1 & 0.44 & 1.36 \\ 2.33 & 0 & 1 & 0.47 \\ 1.21 & 0.51 & 0.35 & 1 \end{pmatrix}\mathbf{N}). \tag{S5}$$

where $\mathbf{N} = (N_1, N_2, N_3, N_4)$ is the vector of species abundances.

Figure S2A shows that the system exhibits chaotic behavior with intrinsic growth rates $\mathbf{r} = (1, 0.72, 1.52, 1.27)$, Figure S2B shows that the system exhibits a point attractor with intrinsic growth rates $\mathbf{r} = (0.1, 5.72, 1.53, 1.27)$, and Figure S2C shows that the system exhibits species extinction with intrinsic growth rates $\mathbf{r} = (0.4, 0.01, 0.1, 2)$. This illustrates the importance of intrinsic growth rates in population dynamics even under the MCT formalism.

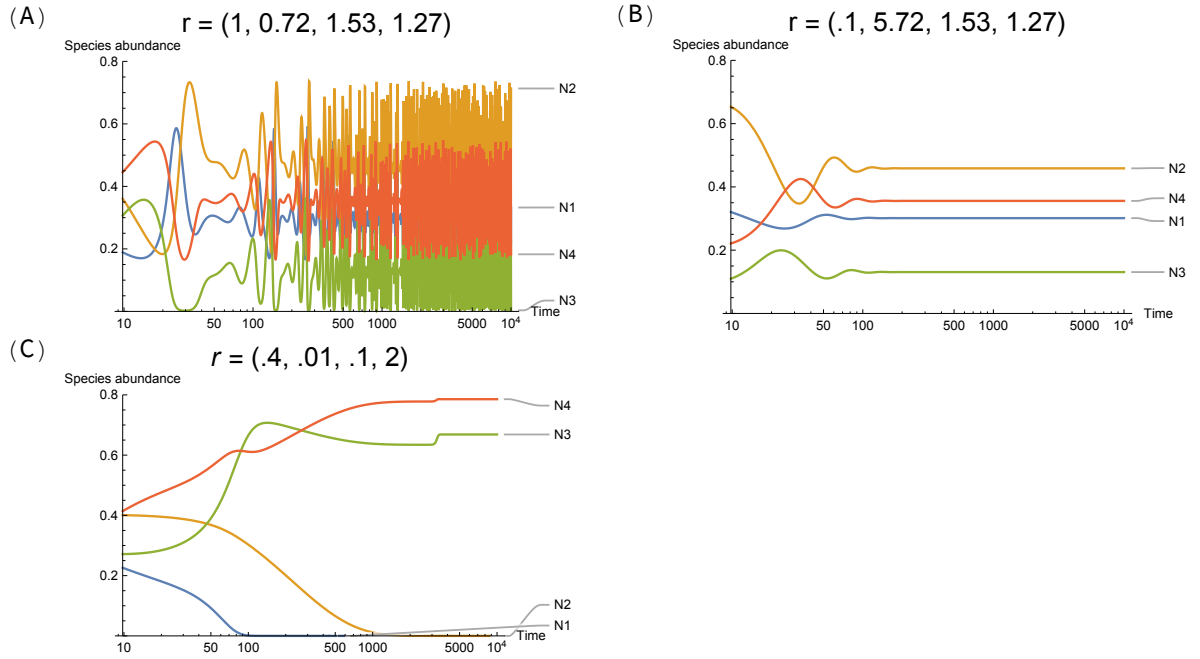

Figure S2: Intrinsic growth rates impact population dynamics. All the simulations are governed by the same initial conditions and the same interaction matrix, but the intrinsic grow rates. Panel A exhibits chaotic behavior, Panel B exhibits a point attractor, and Panel C exhibits species extinction. The x axis is on the log ratio.

C Structural Approach and priority effects

The Structural Approach (SA) has been defined as the structural stability of coexistence under changes in intrinsic growth rates (Saavedra *et al.*, 2017b). Here, we show how SA can be naturally extended to priority effects.

Theorem S1. *The structural stability of priority effects under changes in intrinsic growth rates can be computed as* $\Omega = \arccos \frac{Q_1+Q_2}{\sqrt{1+Q_1^2}\sqrt{1+Q_2^2}}$

Proof. Criteria for stable coexistence is

$$Q_1 < \frac{r_2}{r_1} < \frac{1}{Q_2} \tag{S6}$$

and the criteria for priority effects is

$$\frac{1}{Q_2} < \frac{r_2}{r_1} < Q_1 \tag{S7}$$

Thus, the transition from stable coexistence to priority effects can be seen as

$$\frac{1}{Q_2} \quad \mapsto \quad Q_1 \tag{S8}$$

$$Q_1 \quad \mapsto \quad \frac{1}{Q_2} \tag{S9}$$

With the triangulate equality that

$$\frac{\tan\alpha - \tan\beta}{1+\tan\alpha\tan\beta} = \frac{1/\tan\beta - 1/\tan\alpha}{1+1/(\tan\alpha\tan\beta)} \tag{S10}$$

This shows that the normalized solid angle Ω remains the same after the transition. With elementary trigonometric transformation, we have the result shown in Fig. S3. □

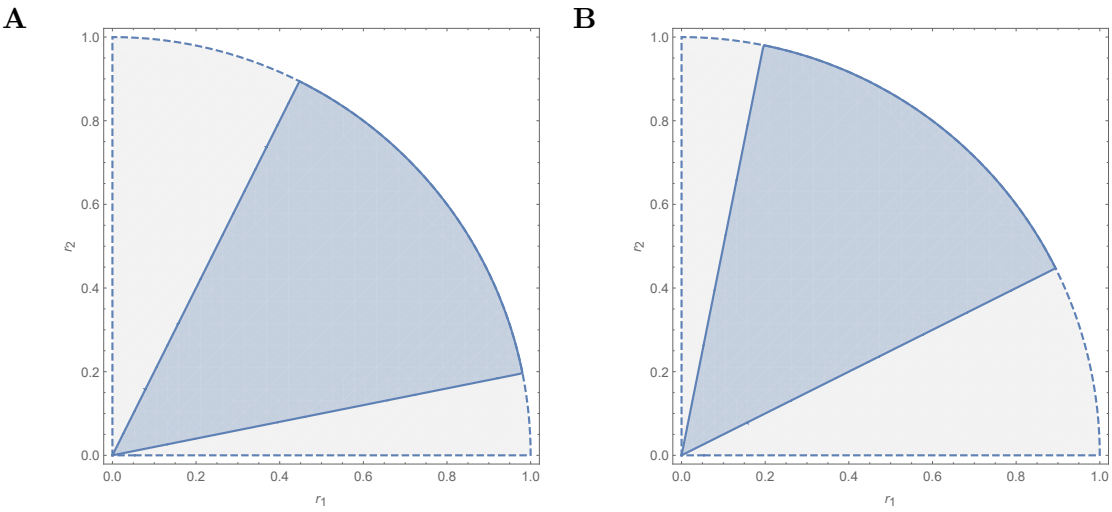

Figure S3: Cartoon of the proof. The figure shows how the transformation alters the relative position of the structural stability region but keeps the size fixed. Panel A represents coexistence, while Panel B represents priority effects.

D Formal combination of MCT and SA

To simplify the derivation of the combination of MCT and SA, let us denote the fitness ratio $\frac{r_2}{r_1}\sqrt{\frac{Q_2}{Q_1}}$ as ϕ and the ratio of intrinsic growth rates $\frac{r_2}{r_1}$ as μ.

D.1 Stabilizing mechanism and SA

Let us fix the fitness ratio ϕ as a positive constant. Then $Q_2 = \phi^2\mu^{-2}Q_1$, and the niche overlap can be written as

$$\rho = \sqrt{Q_1 Q_2} = \phi\mu^{-1}Q_1, \tag{S11}$$

which implies that

$$\cos\Omega = \frac{\rho(\phi^{-2}\mu^2+1)}{\sqrt{1+\phi^{-2}\mu^2\rho^2}\sqrt{\rho^2+\phi^{-2}u^2}}. \tag{S12}$$

Looking at the conditions in ρ that increase Ω (the region of coexistence or priority effects) we have

$$\frac{\partial\cos\Omega}{\partial\rho} = \frac{\phi^{-2}\mu^2(1-\rho^4)(\phi^{-2}\mu^2+1)}{(\phi^{-2}\mu^2+\rho^2)^{3/2}(\phi^{-2}\mu^2\rho^2+1)^{3/2}}, \text{ which is } \begin{cases} >0, \text{if } \rho<1 \\ <0, \text{if } \rho>1, \end{cases} . \tag{S13}$$

which implies that Ω decreases as niche overlap ρ increases under coexistence ($\rho < 1$), and Ω increases as niche overlap ρ increases under priority effects ($\rho > 1.$). Similarly, looking at the conditions in μ that increase Ω we have

$$\frac{\partial\cos\Omega}{\partial\mu} = \frac{\phi^{-2}\mu\rho(\rho^2-1)^2(\phi^{-2}\mu^2-1)}{(\phi^{-2}\mu^2+\rho^2)^{3/2}(\phi^{-2}\mu^2\rho^2+1)^{3/2}}, \text{ which is } \begin{cases} >0, \text{if } Q_1>Q_2 \\ <0, \text{if } Q_1<Q_2, \end{cases} . \tag{S14}$$

Thus, when $\phi^{-2}\mu^2 > 1$ (i.e., $Q_1 > Q_2$), Ω would increase if $\mu = \frac{r_2}{r_1}$ decreases; and when $\phi^{-2}\mu^2 < 1$ (i.e., $Q_1 < Q_2$), Ω would increase if $\mu = \frac{r_2}{r_1}$ increases. This pattern is the same regardless of whether looking at coexistence or priority effects.

D.2 Equalizing mechanism and SA

Let us fix the niche overlap ρ as a positive constant. Without loss of generality, we assume that fitness ratio $\phi \geq 1$. Then $Q_1 = \rho\mu\phi^{-1}, Q_2 = \rho\mu^{-1}\phi$. Unlike the stabilizing mechanism, the equalizing mechanism is *not* always well-defined as feasibility is not always satisfied — μ has to lie within the feasibility domain spanned by $(Q_1, 1)$ and $(1, Q_2)$. Hence, we define $\Omega := 0$ when feasibility is violated. Focusing on priority effects we have

$$\cos\Omega = \frac{\rho(\mu^2+\phi^2)}{\sqrt{\phi^2+\rho^2\mu^2}\sqrt{\mu^2+\rho^2\phi^2}}, \text{where } \rho^{-1}\mu^2 < \phi < \rho\mu^2 \tag{S15}$$

Note that the condition $\rho^{-1}\mu^2 < \phi < \rho\mu^2$ is equivalent to the feasibility condition $\frac{1}{Q_1} < \mu < Q_2$. Similarly, for coexistence we have

$$\cos\Omega = \frac{\rho(\mu^2+\phi^2)}{\sqrt{\phi^2+\rho^2\mu^2}\sqrt{\mu^2+\rho^2\phi^2}}, \text{where } \rho\mu^2 < \phi < \rho^{-1}\mu^2 \tag{S16}$$

Focusing only on non-trivial Ω (i.e., $\cos\Omega \neq 1$), the derivative of $\cos\Omega$ is

$$\frac{\partial\cos\Omega}{\partial\phi} = \frac{\mu^2\rho(\rho^2-1)^2\phi(\phi^2-\mu^2)}{(\mu^2\rho^2+\phi^2)^{3/2}(\mu^2+\rho^2\phi^2)^{3/2}}, \tag{S17}$$

which impels that Ω decreases when $\phi > \mu$ and increases otherwise in both coexistence and priority effects.

Furthermore, when Ω are fixed, then

$$\phi^2 = \frac{\mu^2 \csc^2(\Omega)\left(2(\rho^4+1)\cos^2(\Omega) - 4\rho^2 + \sqrt{2}(\rho^2-1)\cos(\Omega)\sqrt{\rho^4 + (\rho^2+1)^2\cos(2\Omega) - 6\rho^2 + 1}\right)}{4\rho^2}. \tag{S18}$$

The conditions above imply that Q_1 and Q_2 do not depend on μ. Note that in the extreme case when Ω reaches its maximum (i.e., $\phi = \mu$, or, equivalently, $Q_1 = Q_2$), the maximum of Ω is $\arccos\left(\frac{2\rho}{\rho^2+1}\right)$, which only depends on the niche overlap ρ.

E Ratios of intrinsic growth rates and maximum solid angle

Figure 4 shows that different ratios of intrinsic growth rates r_2/r_1 can yield the same maximum solid angle Ω. While different ratios of intrinsic growth rates r_2/r_1 would have the same aggregated tolerance to random perturbations (i.e. Ω), they have different tolerances to directional perturbations. Figure S4 shows the three ratios $r_2/r_1 = 1, 2, 10$ with their associated maximum Ω. When $r_2/r_1 = 1$, the tolerances to directional perturbations (i.e. distances to the boundaries) are similar. However, when r_2/r_1 increases, the tolerances to directional perturbations shows a stronger trade-off.

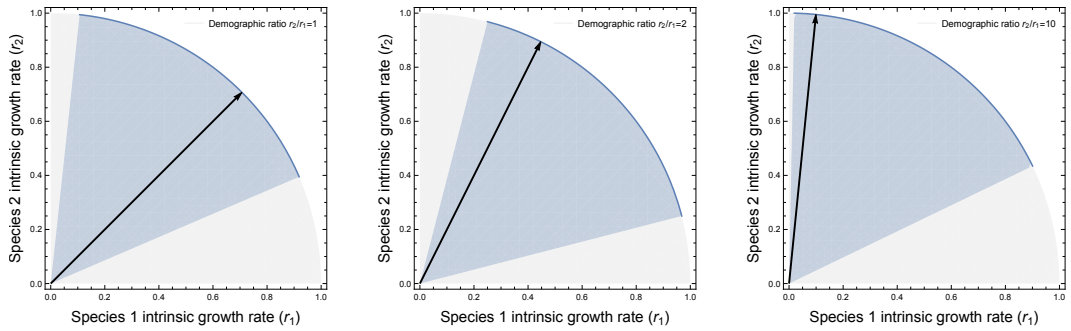

Figure S4: Different tolerances to directional perturbations with the same Ω. The two axes denote the intrinsic growth rates of two species. The blue region denotes the feasibility domain. The black line denotes the ratio of intrinsic growth rates (values in upper-right). As the ratio of intrinsic growth rates deviates more from 1, the system is more robust to perturbation upon one boundary and less robust to perturbation upon the other boundary.

F Annual plant model

This section discusses how to apply MCT and SA on an the annual plant model (Godoy & Levine, 2014). A more detailed disucssion can be found in Godoy & Levine (2014); Godoy *et al.* (2014); Saavedra *et al.* (2017b). The annual plant model reads as

$$\frac{\mathrm{d}N_{i,t+1}}{\mathrm{d}t} = (1-g_i)s_iN_{i,t} + \frac{g_i\lambda_iN_{i,t}}{1+\sum_{j=1}^{n}\tilde{\alpha}_{ij}g_jN_{j,t}}, \tag{S19}$$

where g_i is the germination rate, s_i is the seed survival probability, λ_i is the fecundity rate, and $\tilde{\alpha}_{ij}$ is the competition strength (relative reduction in per capita growth rate). After algebraic manipulation, the equilibrium N_i^* can be expressed as a linear equation:

$$\frac{g_i\lambda}{1-(1-g_i)s_i} - 1 = \sum_{j=1}^{n}\tilde{\alpha}_{ij}g_jN_j^*. \tag{S20}$$

Then, Eq. 1 can be achieved via re-parametrization

$$r_i \coloneqq \frac{g_i\lambda}{1-(1-g_i)s_i} - 1 \tag{S21}$$

$$\alpha_{ij} \coloneqq \tilde{\alpha}_{ij}g_j \tag{S22}$$

G Hypothesis testing for field data

Here we performed a hypothesis testing to show that there is a significant statistical tendency to increase the feasibility domain Ω rather than increasing the fitness equivalence in the field data (Figure 5B-C). Recall that the maximization of the former implies higher pressures in intrinsic growth rates, while the maximization of the latter implies higher pressures in competition strengths. Specifically, we established two hypotheses:

$$H_0: \quad \text{the tolerance to perturbation in competition strength is maximized} \tag{S23}$$
$$H_1: \quad \text{the tolerance to perturbation in intrinsic growth rates is maximized} \tag{S24}$$
$$\tag{S25}$$

To formalize this problem, it is equivalent to ask whether points in Figure 5B-C are closer to the fitness equivalence line or to the maximizing Ω line. Let us denote the distance to the fitness equivalence line as d_1 and the distance to the maximizing Ω line as d_2. Then, the hypotheses are equivalent to

$$H_0: \quad d_2/d_1 < 1 \tag{S26}$$
$$H_1: \quad d_2/d_1 > 1 \tag{S27}$$

Figure S5 shows the distribution of the log ratios of distances d_2/d_1 in the empirical data set. Then, we ran Wilcoxon signed-rank test on the two hypotheses. For coexistence, we found that H_0 has a p value of 1 and H_1 has a p value of 3.049×10^{-7}. Similalry, for priority effects, we found that H_0 has a p value of 1, and H_0 has a p of value 0.0001009. Therefore, we rejected the null hypothesis, and concluded there is a tendency to maximize the tolerance to perturbations in intrinsic growth rates.

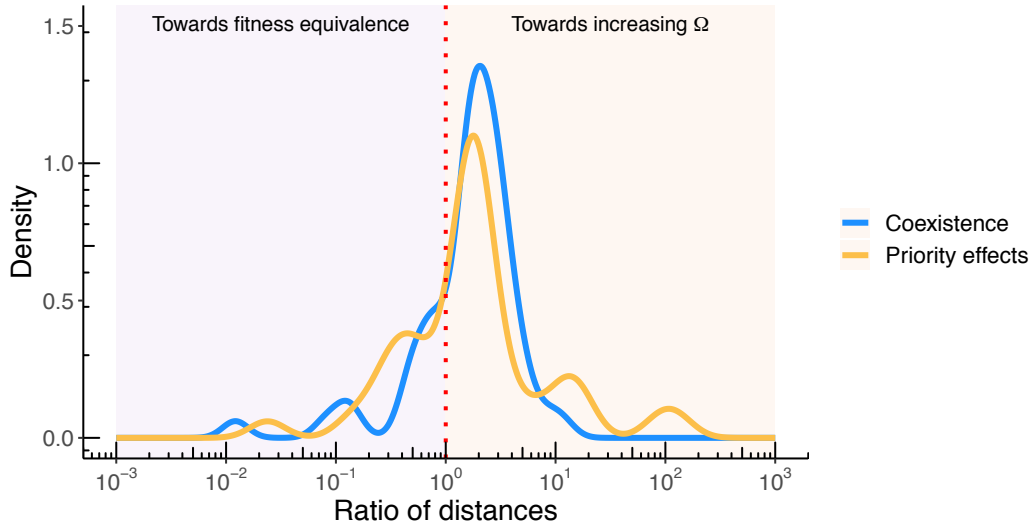

Figure S5: This figure shows the distribution of the ratio of distances d_2/d_1 for coexistence (in blue) and priority effects (in orange) in the annual plants assemblages. The dotted red line denotes the equal distance $d_1 = d_2$. The ratio of distances is plotted on log ratios.